Spatial Audio Cueing Algorithms for Augmented Pilot Perception in Degraded/Denied Visual Environments

Michael T. Morcos
Graduate Research Assistant
Spencer M. Fishman
Graduate Research Assistant
Umberto Saetti
Assistant Professor
Department of Aerospace Engineering
University of Maryland
College Park, MD 20740

Tom Berger
Flight Controls Group Lead
U.S. Army Combat Capabilities Development
Command Aviation & Missile
Moffett Field, CA 94035

Martine Godfroy-Cooper
Senior Research Psychologist
Edward N. Bachelder
Senior Research Engineer
San Jose State University
Moffett Field, CA 94035

ABSTRACT

This paper demonstrates the development, implementation, and testing of spatial audio cueing algorithms for augmented pilot perception. Cueing algorithms are developed for roll-axis compensatory tracking tasks where the pilot acts on the displayed error between a desired input and the comparable vehicle output motion to produce a control action. The error is displayed to the pilot using three different cueing modalities: visual, audio, and combined visual and audio. For the visual and combined visual and audio modalities, visual cues are also considered in degraded visual environments (DVE). Spatial audio algorithms that are based on a proportional-derivative (PD) compensation strategy on the tracking error are found to provide satisfactory pilot vehicle system (PVS) performance for the task in consideration when using audio feedback only (no visual cues) and to improve PVS performance in DVE when using combined visual and audio feedback. These results are in line with previous studies on the use of full-body haptics for augmented pilot perception. The combination of these results indicate that the use of secondary sensory cues such as full-body haptics and spatial audio to augment the pilot perception can lead to improved/partially-restored PVS performance when primary sensory cues like vision are impaired or denied.

INTRODUCTION

In symbiotic piloting, a human pilot shares perception and control authority with an artificial intelligence (AI) agent to control the motion of a vehicle, acting as a symbiotic organism (Fig. 1). Here, a vehicle is intended as any generic n-DOF machine (*e.g.*, airplanes and helicopters, drones, *etc.*) that can move across regions of physical space. The vehicle may physically host or be teleoperated by a human pilot, and its dynamics are augmented by an AI agent with human-like perception and actuation dynamics. Current perception models for symbiotic human-machine piloting of vehicles are based on the dominant visual (*i.e.*, sight) and vestibular (*i.e.*, equilibrium) cues, but neglect less dominant perception cues, such as somatosensory cues (*e.g.*, haptics) or auditory cues (*e.g.*, 3-D audio), and interactions between primary and secondary sensory channels. As such, there is limited understanding on shared human-machine perception solutions for vehicle piloting when the symbiotic system operates with denied/impaired sensory channels (*e.g.*, degraded visual environment), denied/impaired interactions between sensory channels, or with primary sensory channels augmented with traditionally secondary perception cues.

Denial or impairment of perceptual channels may arise from environmental conditions (*e.g.*, weather), factors limiting machine abilities (*e.g.*, sensor failure), or human pilot abilities (*e.g.*, temporary or permanent disabilities, *e.g.*, fatigue). Within the context of manned piloting of aircraft, modeling of secondary sensory cues could help develop cueing strategies to enable emergent pilot vehicle system (PVS) performance,

Presented at the 49th European Rotorcraft Forum, Bückeburg, Germany, September 5–7, 2023.

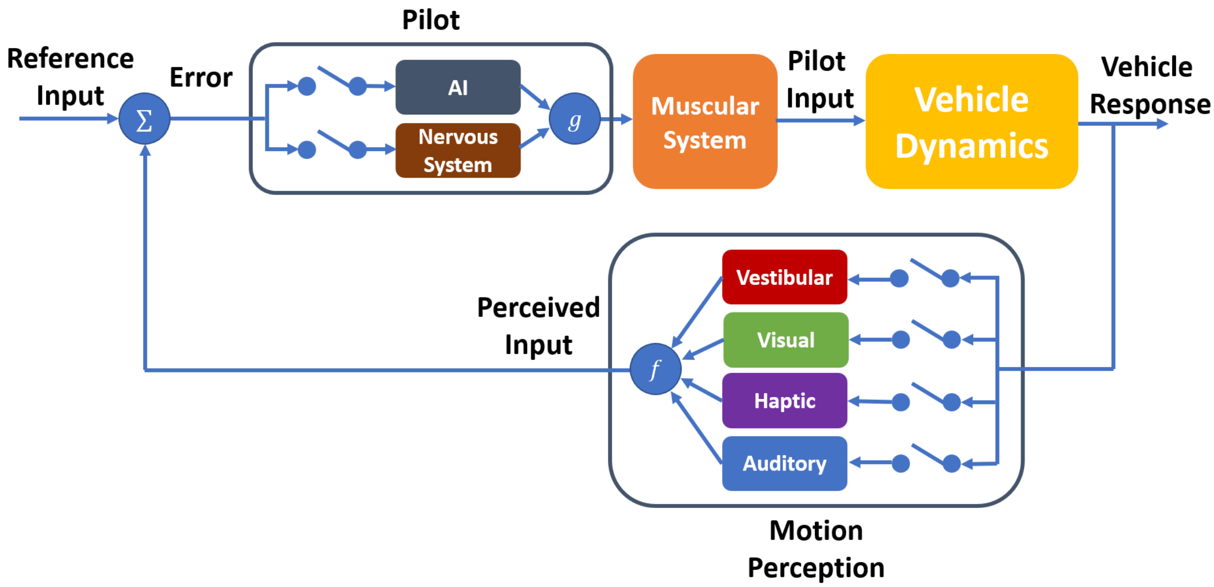

Fig. 1: Symbiotic pilot vehicle system.

or to supplement for pilot spatial disorientation which may be caused by temporary or permanent loss/malfunction of their vestibular and/or visual systems.

Within the context of secondary sensory cueing, previous studies have shown that full-body tactile cueing of the relative motion of a hovering helicopter with respect to a target fixed in space is an effective strategy to increase spatial awareness and handling qualities, and decrease pilot workload in and out of degraded visual environment (DVE). In these studies, the relative linear and angular positions, velocities, and accelerations were cued to the pilot through an array of tactors, and using tactor pulse patterns with varying amplitude, frequency, and waveform (Refs. 1–4). Recently, full-body haptics in the form of electrical muscular stimulation (EMS) was investigated for augmented pilot perception in degraded/denied visual environments (Ref. 5). Contrary to previous studies, these haptic cueing algorithms used are based on a continuous cueing strategy rather than on a binning strategy. Similar strategies to those of Refs. 1,2,5 could be used in the proposed investigation and adapted through spatial audio cueing.

As such, the objectives of the present investigation are threefold. The first objective is to extend the crossover model (Ref. 6) to secondary sensory cueing paths like spatial audio cueing. The second objective is to develop efficient spatial audio cueing strategies that can be used in compensatory tracking experiments (Refs. 6, 7) in place of, or in combination with, visual cues. The third objective is to test spatial audio cueing strategies and identify the corresponding PVS dynamics. Comparisons between visual, audio, and combined visual and audio cueing will help understand the potential differences in pilot equalization when leveraging this secondary sensory path to control the motion of an aircraft. Moreover, these experiments will shed light on potential benefits of spatial audio cueing.

The paper begins with a discussion of the overall methodology adopted in this investigation, including an overview of pilot modeling. This is followed by a description of the equipment adopted for the experimental studies. Next, the development and implementation of spatial audio cueing strategies that make use of proportional-derivative compensation are described in detail. Discussions on experiment design and parametric identification from input-output experimental data follows. Results feature both time- and frequency-domain analyses of the experimental data. Quantitative data from the experiments is compared to qualitative data from pilot feedback. Final remarks summarize the overall findings of the study and future developments are identified.

METHODOLOGY

Overview

The present effort focuses on closed-loop compensatory tracking tasks in which the pilot acts on the displayed error e between a desired command input i and the comparable vehicle output motion m to produce a control action c. Historically, information about the error e was presented to the pilot through visual displays, examples of which is shown in Fig. 2 (Ref. 7). In Fig. 2a, the green bar with the inner and outer reticles is aircraft pitch attitude indicator m, whereas the orange bar represents the commanded attitude i. This kind of display is used for pursuit tracking tasks (Ref. 8). The difference between these two is error that the pilot attempts to minimize within the defined desired and adequate performance constraints. These constraints are given by the inner and outer reticles, respectively. Figure 2b shows another kind of visual display used for compensatory tracking tasks referred to as *bow tie* display. This particular display is used to cue roll and pitch attitude errors simultaneously. For pitch-axis evaluations with this display, the objective is to capture and hold the green dot within the magenta circles for each commanded pitch attitude. For roll-axis evaluations with the same display, the objective is to capture and hold the green line within the bow tie bounds for each commanded bank angle. The idea behind this research is to replace and/or augment these visual displays with spatial audio displays. More specifically, the auditory display will make use of 3-D spatialized sound where headphones cue stereo sound making use of right and left channels.

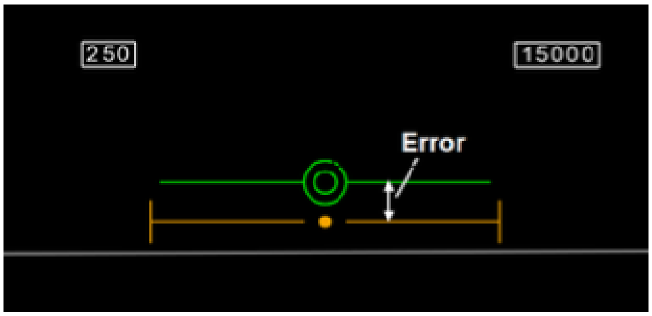

(a) Pitch axis pursuit tracking display.

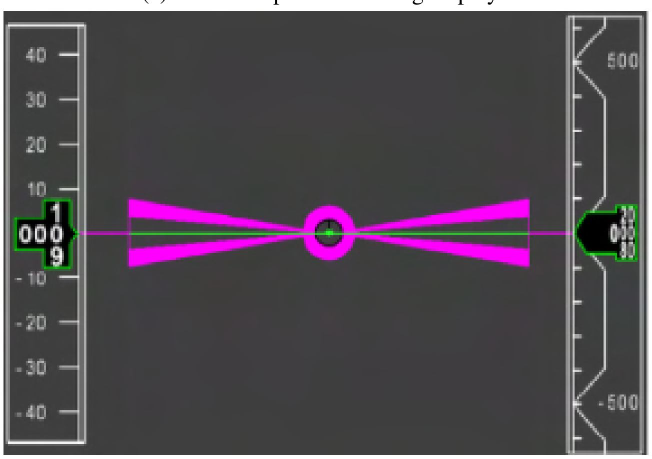

(b) Bow tie display for roll and pitch compensatory tracking tasks.

Fig. 2: Visual displays.

Pilot Vehicle System Modeling

As the base for the prediction of PVS performance and identification of the PVS dynamics, a pilot model structure needs to be specified. Due to the preliminary nature of the investigation, a crossover model (Ref. 9) is assumed as it constitutes a simple yet powerful way to represent the combined PVS dynamics. The PVS dynamics in a compensatory tracking task is shown qualitatively in Fig. 3.

In this study, the vehicle and display dynamics are all combined into the controlled element with a transfer function $Y_c(s)$. The portion of the pilot's control action linearly correlated with the input is represented by the quasi-linear describing function $Y_p(s)$, which also includes the effects of the manipulator characteristics. In a compensatory control task, it was shown through extensive research (see, *e.g.*, Ref. 6) that the human pilot adapts his or her dynamics so that near crossover frequency ω_c (*i.e.*, where $|Y_pY_c| = 1$, or 0 dB) the open-loop dynamics are given by:

$$Y_{OL}(s) = Y_pY_c = \frac{\omega_c}{s}e^{-s\tau_e} \tag{1}$$

where τ_e is the effective time delay, including transport delays and neuromuscular lags. It is worth noting that the crossover frequency is equivalent to the loop gain and accounts for the pilot's adaptive compensation for the controlled element gain. The aircraft dynamics is assumed to have the following general form:

$$Y_c(s) = \frac{K_e}{s\,(T_Is+1)} \tag{2}$$

and is representative of the roll attitude response to the pilot lateral stick. The simplest pilot describing function form for this particular aircraft dynamics, which corresponds to the open-loop crossover model, is:

$$Y_p(s) = K_p(T_Ls+1)e^{-s\tau_e} \tag{3}$$

where K_p is the pilot static gain and T_L is the pilot lead time constant. It is worth mentioning that Ref. 6 suggests the pilot lead time to be approximately equal to the lag time constant τ_I of the aircraft dynamics. This way, the pilot can adjust his or her gain K_p to place the crossover frequency where required to complete the task. Thus, given known aircraft dynamics, the human pilot parameters to be identified for each cueing modality are K_p and τ_e. Moreover, particular focus is be placed on estimating and comparing ω_c for each cueing modality.

If a sensory modality and/or vehicle configuration yields a high crossover frequency, *i.e.*, $\omega_c > 4$ rad/s (high performance) the pilot's neuromuscular mode will start to influence the open-loop response such that the latter can become much flatter than what the crossover model predicts. In this case, the pilot model proposed in Ref. 10 should be used, which accounts for the neuromuscular dynamics.

EQUIPMENT

Spatial audio cueing is achieved through a closed-ear gaming headset (Logitech Pro-G 50 mm), shown in Fig. 4. This headset is equipped with a hybrid mesh PRO-G driver measuring 1.97 inches (50 mm), ensuring good sound quality across a frequency range of 20 Hz to 20 kHz. With an impedance of 35 Ohms and a sensitivity of 91.7 dB SPL at 1 mW and 1 cm, this headphone provides a balanced and immersive listening experience for users.

The controller used for tracking task is a Logitech X52 Pro joystick, shown in Fig. 5. The joystick has three degrees of freedom: left/right, fore/aft, and twist. The joystick adopts a base spring with constant stiffness.

AUDIO CUEING STRATEGY

A hybrid continuous-binning cueing of the roll attitude tracking error and/or its time derivative is found to be an effective audio cueing strategy. The general form of this strategy is a

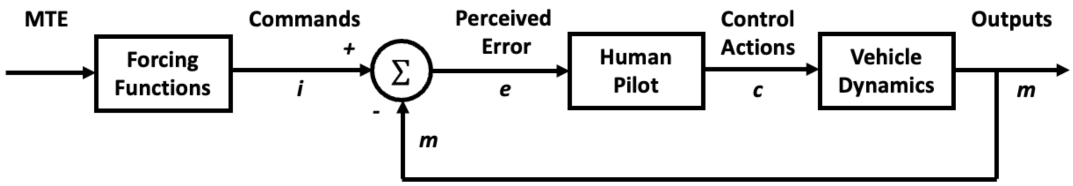

Fig. 3: Pilot vehicle system in a compensatory tracking task.

Fig. 4: Logitech Pro Gaming Headset

(a) Front. (b) Side.

Fig. 5: Logitech X52 Pro joystick.

proportional-derivative (PD) compensation on the roll attitude tracking error:

$$M = K_\mathrm{P} e_\phi + K_\mathrm{D} \dot{e}_\phi \tag{4}$$

where M is a parameter representing the displayed error and e_ϕ is the roll attitude tracking error. The attitude tracking error is defined as the difference between the commanded and displayed roll angles $e_\phi = \phi_\mathrm{cmd} - \phi_\mathrm{dis}$. Within the context of Fig. 3, the displayed error e corresponds to e_ϕ, the desired command input i is ϕ_cmd and the vehicle output motion m is represented by ϕ. Note that in this compensatory tracking task $\phi_\mathrm{cmd} = 0$, such that effectively $e_\phi = \phi_\mathrm{dis}$. The displayed bank angle is given by the difference between the actual bank attitude and some disturbance, such that $\phi_\mathrm{dis} = \phi - \phi_\mathrm{SOS}$. The disturbance is given by a sum of sines (SOS) signal and will be discussed later in the paper. Additionally, K_P and K_D are the proportional and derivative gains, respectively. It is worth noting that the audio gain is adjusted for each subject based on their perception of sound. The maximum gain corresponds to the maximum stimulus that is perceived by the pilot as not annoying and harmful to the ear. The proportional gain is tuned based on the error bounds for Desired and Adequate performance (discussed later in the paper). The proportional gain K_P is chosen to give $M = 50\%$ at the Desired error threshold of 5 deg and $M = 100\%$ at the Adequate error tolerance threshold of 10 deg. This implies $K_\mathrm{P} = 10\%/deg$ and is found by:

$$K_\mathrm{P} = \frac{(\mathrm{SR}_\mathrm{max} - \mathrm{SR}_\mathrm{min})}{e_{\phi_\mathrm{Ade}} - e_{\phi_\mathrm{Des}}} \tag{5}$$

where $\mathrm{SR}_\mathrm{max} = 100\%$ and $\mathrm{SR}_\mathrm{min} = 50\%$. This way, the displayed error M will reach 100% if for $e_\phi = e_{\phi_\mathrm{Ade}}$. The derivative gain is tuned by trial and error. An integral gain was not found to yield any particular benefits to the cueing strategy and was therefore discarded. The azimuth location and sound wave frequency to be generated depend, respectively, on the sign and the magnitude of M. When $M > 0$, a sound signal is played at the right ear whereas for $M < 0$ a sound signal is played at the left ear. The parameter M is then used to calculate the frequency of the sound generated by the OpenAL library. The sample rate is 44100 Hz and the pulse duration is set to 0.03 sec. Based on this strategy, the pilot will perceive a sound in the direction of the error or, equivalently, in the verse of the control action to be taken to reduce the error. The sound signal amplitude is given by:

$$A = \sin(2\pi\omega t) \tag{6}$$

where ω is the sound signal frequency. The sound frequency is chosen via a binning strategy consisting of five frequency bins. These bins are chosen so as to make the jump between each bin easily perceivable by the pilot. The relation between the displayed frequency and M is exponential for the three middle levels and constant for the lower and upper levels as described in Table 1. Moreover, sound signals are cued in pulses for low and mid values of M with a fixed pulse width and a linearly varying inter-pulse interval. For higher values of M, the inter-pulse interval is zero (*i.e.*, no time gap between pulses). As such, the refresh rate of the audio signal is the summation of the pulse width and the inter-pulse interval, resulting in an adaptive proportional relation with respect to the value of the error and error rate.

A bow tie display for compensatory tracking task is used in this research. Three visual indicators are used as symbology and are shown in Fig. 6. The green line corresponds to the displayed bank angle. The orange line represents the desired bank angle. The magenta lines indicate the boundaries for Desired and Adequate performance. More specifically, the inner portion boundary of the magenta indicator corresponds to the Desired performance boundary, whereas the outer portion corresponds to the Adequate performance threshold. The displayed bank attitude is the difference between the actual roll attitude and the disturbance from the sum-of-sines (SOS) forcing function described in the next section:

$$\phi_{\text{dis}} = \phi - \phi_{\text{SOS}} \tag{7}$$

Note that the command indicator value corresponds to the fixed horizon reference.

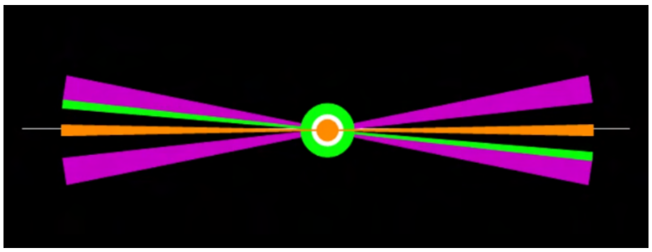

Fig. 6: Bow tie display

Consider the case shown in Fig. 6, where the displayed bank angle is $\phi_{\text{dis}} = 5$ deg. Also, assume zero roll rate error, *i.e.*, $\dot{e}_\phi = 0$. Then, a proportional gain $K_{\text{P}} = 9$ yields $M = -45\%$. According to the binning strategy, this results in a Level 3 frequency range, with $\omega = 1231.14$ Hz and an inter-pulse interval equals to 0.11 sec. Since $M < 0$, the sound signal is cued to the pilot in their left ear (*i.e.*, with an azimuth $\psi = -90$ deg). This prompts the pilot to make a left stick correction to compensate for the error and bring the aircraft back to level. This cueing strategy is summarized in Table 1. This audio cueing strategy build on the work in Ref. 11.

EXPERIMENT DESIGN

The set of experiments object of this study involve a precision, non-aggressive, closed-loop compensatory tracking task in the roll axis only where the forcing function (disturbance/command input) is chosen to be a sum of signs (SOS), as per Ref. 7. The SOS forcing function is used to drive the compensatory tracking task through which the pilot attempts to minimize the displayed error within desired performance constraints. A Fibonacci series-based SOS input is designed to emphasize the frequency range that encompasses key vehicle dynamics and typical human pilot control action, ranging from 0.3 to approximately 6 rad/s. The length for scoring time is 60 seconds, preceded by a 10 sec ramp up and followed by 5 sec ramp down period. Five trials are conducted for each cueing modality. Each of these five trials uses a different SOS signal, where the sum of sines are based on randomly-generated phasing angles and stored offline. The five SOS time histories are the same across each cueing modality and are presented to the test subject in the same order. Experiments make use of four different subjects, one of which is a test pilot. Each subject performed one practice run before recording the five different patterns for each modality tested. Desired performance is defined such that the tracking error on the roll attitude be less than 5 deg for at least 50% of the scoring time. Adequate performance requires the roll attitude tracking error to be less than 10 deg for at least 75% of the scoring time. These requirements are summarized in Table 2.

The joystick is positioned between the legs of the test subject, whom are seated with their eyes at approximately 1 m from the computer screen. The central positioning of the joystick is justified by the effort in replicating the use of a cyclic stick in a conventional helicopter. By the same rationale, the vertical position of the joystick is adjusted to have the test subjects rest their elbow on their thigh when operating the joystick. This setup is shown in Fig. 7.

Fig. 7: Experimental setup.

The following five cueing modalities are tested:

1. **Visual**: The pilot performs the compensatory tracking task by looking at the visual display only, where the visual display is the bow tie display shown in Fig. 6.

2. **Visual DVE**: Here, visual cues are disturbed by the use of foggles to simulate DVE.

3. **Visual + Audio**: Information about the tracking error is provided to the pilot via the visual (bow tie) display and via spatial audio cueing. The cueing adopts proportional-derivative compensation.

4. **Visual DVE + Audio**: This is similar to the cueing modality above, but visual cues are disturbed by the use of foggles.

5. **Audio**: Information about the tracking error is provided to the pilot via spatial audio cueing only while the pilot is blindfolded (Fig. 7). Cueing adopts proportional-derivative compensation.

This test matrix is summarized in Table 3. It is worth noting that derivative-only compensation was discarded a priori as test subjects incurred in pilot-induced oscillations (PIOs).

Table 1: Audio cueing strategy.

Threshold	Frequency [Hz]	Condition on Frequency [%]	Pulse-Width [sec]	Inter-Pulse Interval [sec]	Condition on Inter-Pulse Interval [%]
Level 1	110	$0 < \|M\| < 5$	0.03	$-0.002\|M\|+0.2$	$0 < \|M\| < 65$
Level 2	$220 \cdot 2^{\left(\frac{\|M\|}{50}\right)}$	$5 \leqslant \|M\| < 30$	0.03	$-0.002\|M\|+0.2$	$0 < \|M\| < 65$
Level 3	$1000 \cdot 2^{\left(\frac{\|M\|-30}{50}\right)}$	$30 \leqslant \|M\| < 100$	0.03	0	$\|M\| \geq 65$
Level 4	$2880 \cdot 2^{\left(\frac{\|M\|-100}{50}\right)}$	$100 \leqslant \|M\| < 150$	0.03	0	$\|M\| \geq 65$
Level 5	6880	$\|M\| \geq 150$	0.03	0	$\|M\| \geq 65$

Table 2: Desired and Adequate performance metrics.

Performance	Tracking Error Bounds [deg]	Scoring Time [%]
Desired	$\|e_\phi\| < 5$	≥ 50
Adequate	$\|e_\phi\| < 10$	≥ 75

Additionally, proportional-only compensation was also discarded a priori in light of the results of Ref. 5. In this study, PD compensation was shown to yield higher performance than P-only compensation. The aircraft dynamics is chosen to be representative of the roll dynamics of a conventional utility helicopter similar to a UH-60 with Level 1 handling qualities. The specific transfer function used in this study is:

$$Y_c(s) = \frac{\phi}{\delta_{lat}}(s) = \frac{L_{\delta_{lat}}}{s\,(s - L_p)} \tag{8}$$

where $L_p = -3.5$ 1/s is the roll acceleration due to the roll rate and $L_{\delta_{lat}} = 0.147$ 1/(s^2-%) is the roll acceleration due to a lateral stick displacement. The SOS code and visual cueing interface of Ref. 7 are developed in C/C++, along with interface between these two, the spatial audio OpenAL library, and the aircraft dynamics. The aircraft dynamics is implemented in MATLAB®/Simulink and subsequently compiled to C/C++ code.

PARAMETRIC IDENTIFICATION

Parametric identification studies make use of the CIFER® (Ref. 12) software tool. The identification procedure is based on a two-step process. First, frequency responses of the aircraft output to the tracking error are extracted from piloted simulation data. Next, state-space models are identified from the frequency response data.

Pilot Vehicle System Dynamics

Consider the PVS dynamics of Eq. (1):

$$Y_{OL}(s) = \frac{\phi}{e_\phi}(s) = \frac{\omega_c}{s} e^{-s\tau_e} \tag{9}$$

To be suitable for state-space parametric identification, these dynamics are transformed into state-space form:

$$\dot{\phi} = [0]\,\phi + [\omega_c]\,e_\phi\,(t - \tau_e) \tag{10}$$

As such, the parameters to be identified from input-output data are ω_c and τ_e.

Pilot Dynamics

Consider now expressing the PVS dynamics of Eq. (1) in terms of the pilot and aircraft dynamics parameters:

$$Y_{OL}(s) = \frac{\phi}{e_\phi}(s) = Y_p Y_c = \frac{L_{\delta_{lat}} K_p (T_L s + 1)}{-L_p s\,(T_I s + 1)} e^{-s\tau_e} \tag{11}$$

$$\approx \frac{L_{\delta_{lat}} K_p}{-L_p s} e^{-s\tau_e} \tag{12}$$

since T_L is approximately equal to T_L (Ref. 6). It is worth noting that $\omega_c = -\frac{L_{\delta_{lat}} K_p}{L_p}$, such that the pilot gain K_p can be identified based on the crossover frequency ω_c identified with the model of Eq. (10).

RESULTS

Pilot Vehicle System Performance

After tuning, the PD gains used for the set of experiments object of this analysis are $K_P = 9$ %/deg and $K_D = 4$ %/(deg-s). The proportional gain stems from Eq. (5) whereas the derivative gain was found via trial and error. Figure 8 shows an example time history for a non-aggressive compensatory

Table 3: Test matrix.

Experiment #	Cueing Modality	K_{P} [%/deg]	K_{D} [%-s/deg]
1	Visual	-	-
2	Visual DVE	-	-
3	Visual + Audio PD	9	4
4	Visual DVE + Audio PD	9	4
5	Audio PD	9	4

tracking task with an audio-only cueing modality and a PD compensation. Figure 8a shows the time history of the roll attitude and roll rate for the same task. Figure 8b shows the time history of the roll rate error and its time derivative.

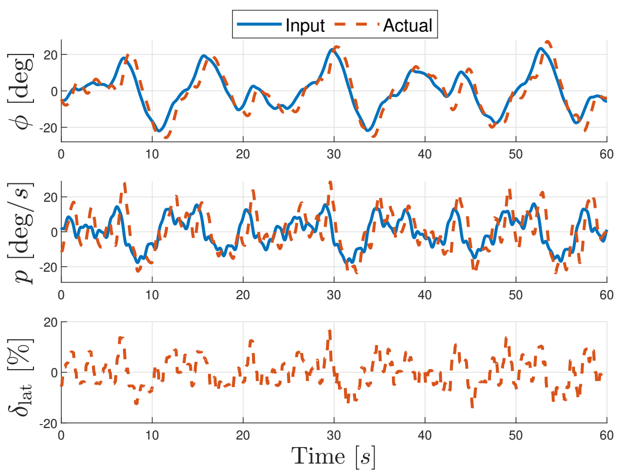

(a) Roll attitude and roll rate.

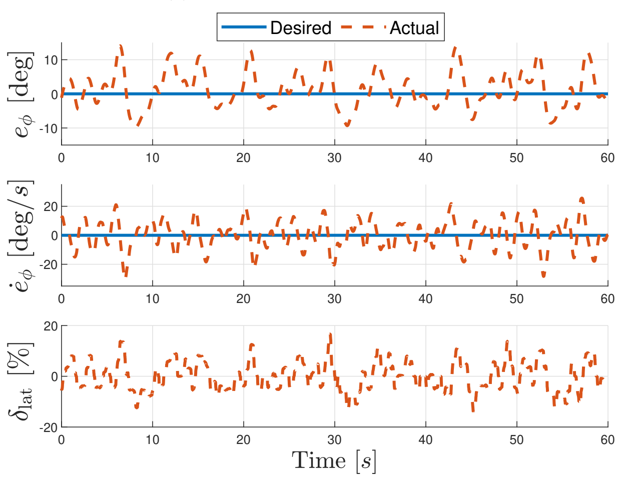

(b) Roll error and error rate.

Fig. 8: Example time history for a non-aggressive compensatory tracking task with audio-only cueing and PD compensation.

The Desired and Adequate performance success rate of each test subject and for each cueing modality are shown in Fig. 9. Desired performance success rates, shown in Fig. 9a, indicate that audio-only cueing adopting PD compensation (light orange boxes) provides satisfactory performance for three out of four test subjects, where the mean performance of test subject not meeting the requirements is still close to the satisfactory threshold. This constitutes a significant result in that it suggests that the task in consideration can be flown without the primary sense of vision, but rather with a secondary perceptual channel like spatial audio. Foggles appear to be an effective strategy to simulate DVE in that desired performance in DVE when using visual-only cueing is significantly degraded (light green and green boxes). Combined visual and audio cueing making use of PD compensation (pink and red boxes) shows a slight increase in performance across all pilots. However, the most accentuated increase in performance is when audio cueing is paired with visual cueing in DVE (red boxes). It is apparent how the performance lost from degraded vision is partially recovered through the use of audio cueing, particularly when using PD compensation. Similar observations can be made for Adequate performance success rates in Fig. 9b.

Figure 10 shows the root-mean-square (RMS) of the roll attitude tracking error. These results further substantiate what is observed in the Desired and Adequate success rate plots. These results suggest that the adoption of spatial audio cueing might be especially useful when visual perception is degraded or denied. On the other hand, pairing audio cues with vision when the latter is not degraded appears to yield only modest improvements.

Identified Pilot Vehicle System Dynamics

While time-domain Desired and Adequate metrics for task performance might be representative of the performance of the spatial audio cueing strategies developed herein, it is important to also perform a frequency-domain analysis to obtain a better understanding of these spatial audio cueing laws. As such, frequency-domain identification is performed both on the open-loop pilot vehicle and on the pilot dynamics. The frequency range used for the identification process is $0.5 \leq \omega_c \leq 4$ rad/s for non-DVE visual-only cueing tasks, $0.5 \leq \omega_c \leq 3$ rad/s for DVE visual and combined visual and audio cueing tasks, and $0.5 \leq \omega_c \leq 2$ rad/s for audio-only cueing tasks. The average cost functions associated with the identification of each cueing modality for each subject were always less than $J = 100$ and typically less than $J = 50$. An average cost function across all cost functions for each frequency response of $J \leq 100$ generally reflects an acceptable

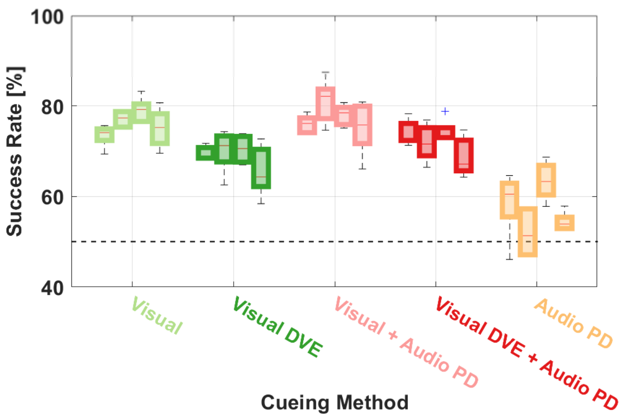

(a) Desired performance.

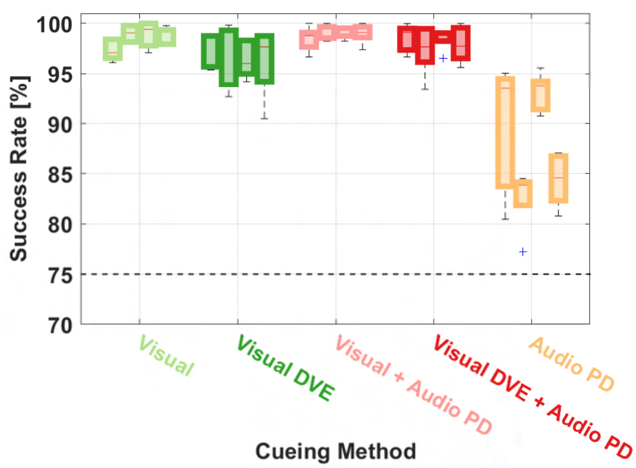

(b) Adequate performance.

Fig. 9: Desired and Adequate performance success rates.

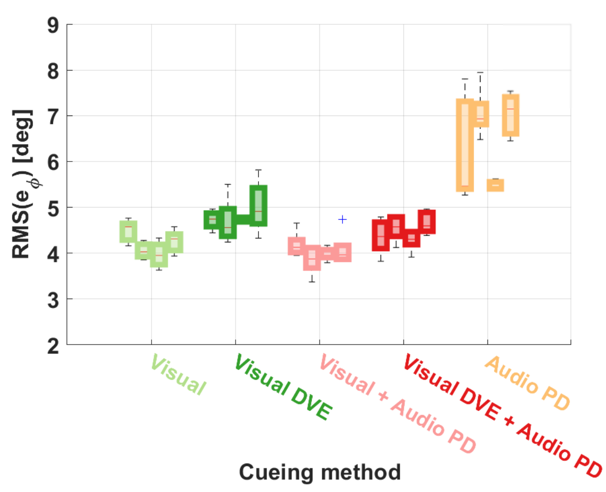

Fig. 10: Root mean square (RMS) of tracking error.

level of accuracy for flight dynamics modeling, whereas a cost function of $J \leq 50$ can be expected to produce a model that is nearly indistinguishable from the original both in the frequency and time domains. However, some of the individual cost functions can reach $J \leq 200$ without resulting in a noticeable loss of overall predictive accuracy (Ref. 12).

Figure 11 shows the identified crossover frequency and effective time delay of the open-loop PVS dynamics. This figure shows that audio-only cueing adopting a proportional-derivative compensation strategy (light orange squares) is associated with high time delays and low crossover frequencies. Visual-only feedback (light green circles) shows low time delays and high crossover frequencies whereas visual-only feedback in DVE (green pluses) shows comparatively higher time delays and lower crossover frequencies. Combined audio PD and visual cueing in non-DVE conditions (pink asterisks) shows slightly higher crossover frequencies than visual-only cueing. The most significant gains are observed for combined visual and audio cueing in DVE conditions (red crosses) when compared to visual-only cueing in DVE, where time delays are lower whereas crossover frequencies are higher.

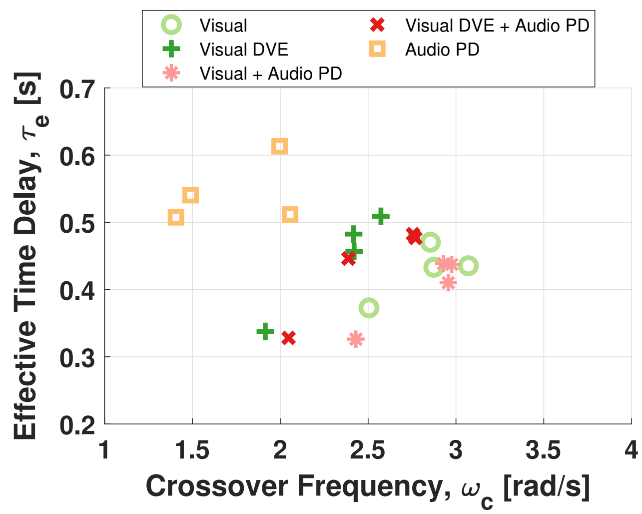

Fig. 11: Crossover frequency and effective time delay of the PVS.

Figure 12 shows the RMS of the identified crossover frequency and effective time delay across all subjects. By looking at Figure 12a one can see the increase in the crossover frequency by the help of audio cueing specially in DVE case. Same analogy can be made to understand the improvements in effective time delay as demonstrated in figure 12b

Figure 13 shows the identified pilot gain and transport delay of the pilot dynamics. These results are in line with those in Fig. 11 as the pilot gains for the pilot and aircraft models in consideration is $K_p = -\frac{\omega_c L_p}{L_{\delta_{lat}}}$. This result is obtained by equating Eq. (1) with the product of Eqs. (2) and (3).

These results are in agreement with the Desired and Adequate success rates, in that audio cueing is particularly useful in restoring lost perception when paired with degraded visual cueing.

Frequency-Domain Analysis

This section focuses on the frequency responses identified from input-output data. The frequency responses shown are

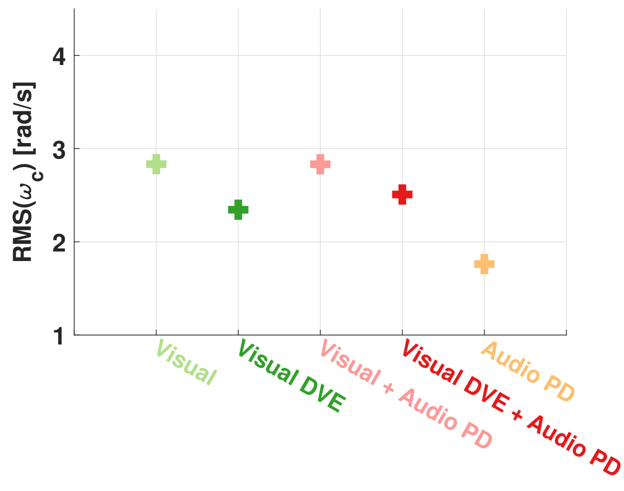

(a) RMS of Crossover frequency

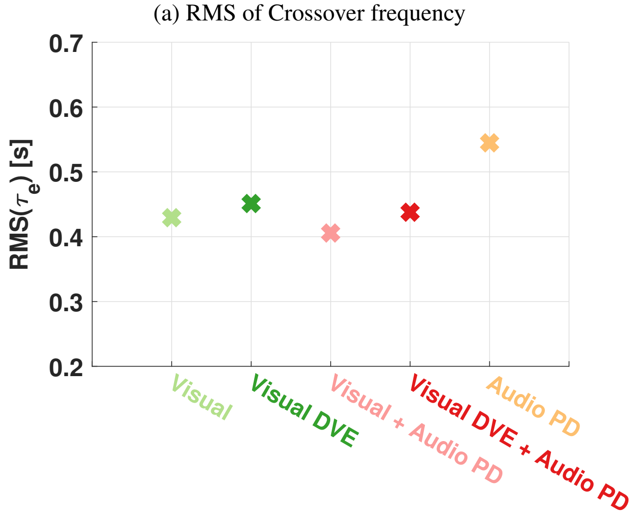

(b) RMS of effective time delay

Fig. 12: RMS of Crossover frequency and effective time delay of the PVS.

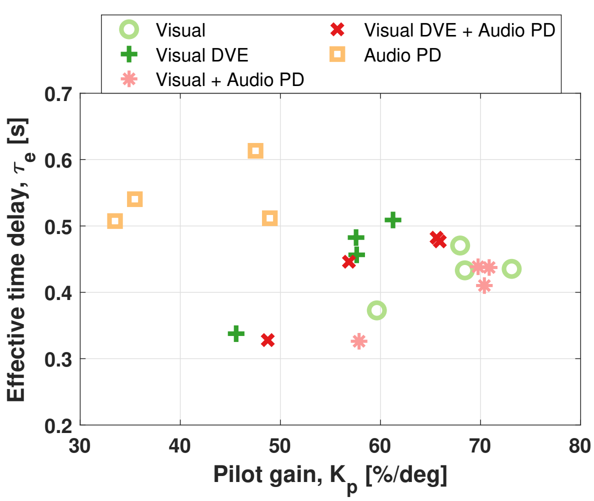

Fig. 13: Pilot gain and transport delay of the PVS.

those for the open-loop pilot vehicle dynamics of Eq. (1), *i.e.*, for $\frac{\phi}{e_\phi}(s)$. These frequency responses are averaged across all pilots to be representative of the mean behavior of all test subjects.

Figure 14 shows the open-loop PVS response for visual-only cueing. Visual cueing in DVE is associated with a lower gain and crossover frequency across the frequency range of interest compared to non-DVE visual cueing. This is indicative of the fact that foggles are an effective way to decrease PVS performance due to the degraded visual perception of the pilot.

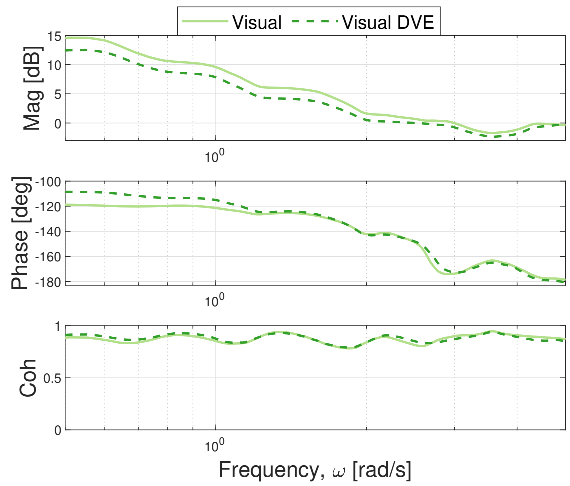

Fig. 14: Averaged frequency responses of the open-loop PVS dynamics for visual-only cueing.

Figure 15 shows the open-loop PVS response for audio-only cueing (PD compensation), non-DVE visual-only cueing, and for combined visual and audio cueing. Audio-only cueing is associated with a low gain across all frequencies of interest when compared to the other strategies, along with a higher phase lag at low frequency. Additionally, spatial audio cueing shows a higher phase lag at frequencies approximately higher than 1 rad/s compared to the other cueing modalities. Combined visual and audio cueing does not seem to significantly affect the gain or phase lag at any frequency. These results suggest that augmenting visual cueing with audio yields no significant improvements when compared to visual-only feedback.

Figure 16 shows the open-loop PVS response for audio-only cueing (PD compensation), non-DVE and DVE visual-only cueing, and for combined visual and audio cueing in DVE. Non-DVE visual-only cueing is associated with the highest gain among all cueing modalities shown whereas audio-only cueing with PD compensation exhibits the lowest gain. Notably, the gain loss stemming from DVE is partially recovered through the use of audio cueing with PD compensation. This suggests that PVS performance lost because of DVE can be partially restored by leveraging secondary sensory cues. In summary, combined visual and spatial audio in DVE yields higher gain than with visual feedback alone. This result further substantiates the results obtained throughout the paper, which indicate that audio feedback may be particularly helpful when visual cues are degraded or denied.

Figure 17 shows the same responses as Fig. 16 but for test

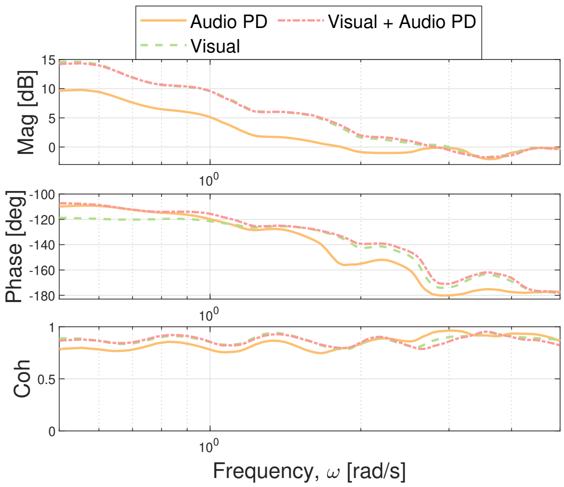

Fig. 15: Averaged frequency responses of the open-loop PVS dynamics for audio-only cueing (PD compensation), non-DVE visual-only cueing, and for combined visual and audio cueing.

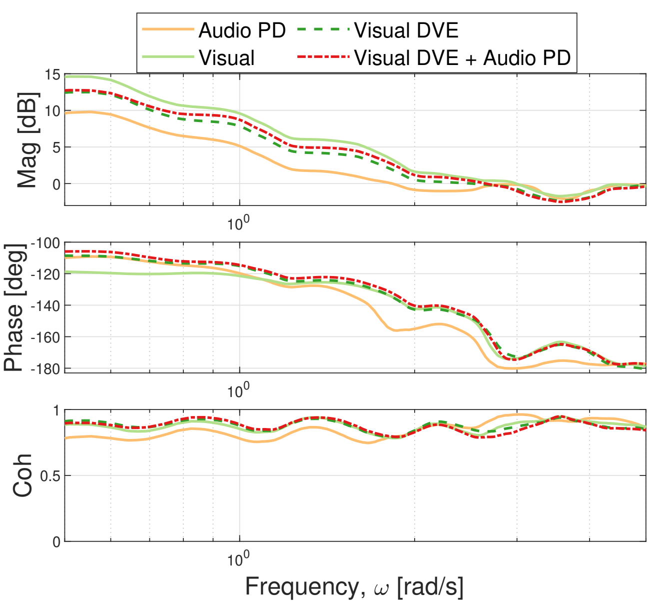

Fig. 16: Averaged frequency responses of the open-loop PVS dynamics for audio-only cueing (PD compensation), non-DVE and DVE visual-only cueing, and for combined visual and audio cueing in DVE.

subject 3 only. According to the results in Figs. 9a and 9b, test subject 3 is the best interpreter of audio-only feedback among all test subjects. Their frequency response is shown to demonstrate that audio-only cueing can provide a comparable response to visual-cueing-only feedback, although with a higher phase lag. Moreover, for this particular test subject, the performance lost for visual-only cueing in DVE is almost entirely recuperated via PD audio cueing.

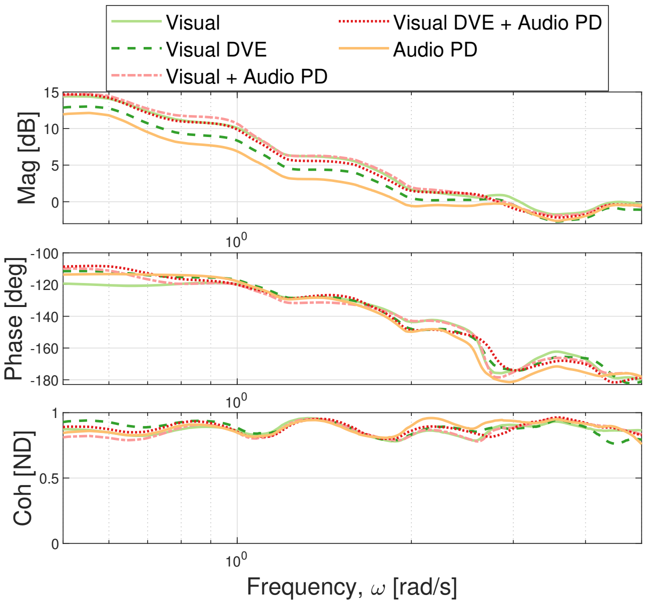

Fig. 17: Test subject 3 frequency responses of the open-loop PVS dynamics for audio-only cueing (PD compensation), non-DVE and DVE visual-only cueing, and for combined visual and audio cueing in DVE.

Identified Crossover Model at Discrete Frequencies

The parameters of the open-loop PVS crossover model of Eq. (1) were identified from the open-loop PVS frequency responses (*e.g.*, Figs. 14 through 17) using only the sum-of-sines frequency where the forcing energy is. Figures 18 and 19 show the crossover frequency and equivalent delay, respectively. As expected based on the performance for the different cueing methods, audio-only cueing with PD compensation has the lowest overall crossover frequency and highest equivalent delay. The highest crossover frequency and lowest delay are seen for combined visual cueing non-DVE and audio PD, which also showed the best overall task performance.

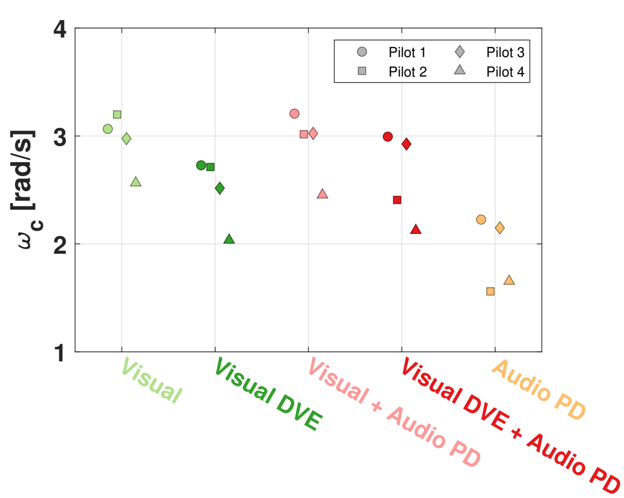

Fig. 18: Identified open-loop PVS crossover frequency.

The PVS stability margins were calculated from the identi-

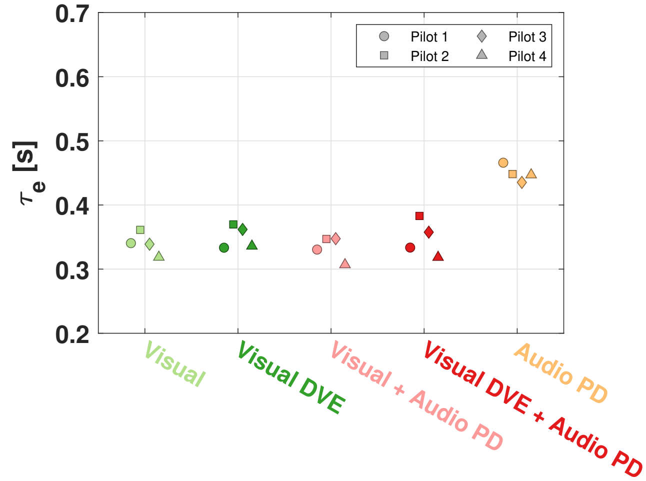

Fig. 19: Identified open-loop PVS equivalent time delay.

fied open-loop PVS crossover model. Figures 20 and 21 show the gain and phase margins of the open-loop PVS system for the different cueing methods, respectively. The mean stability margins are similar for all cases (Gm $\approx$ 5 dB and Pm$\approx$ 35), which are typical numbers for PVS (Ref. 13), and similar to the assumed values used in the ADS-33 (Ref. 14) piloted bandwidth requirements (6 dB and 45 deg). It is clear that the subjects adjust their gain (PVS crossover frequency) based on the equivalent loop delay such that they operate with similar stability margins for all cases. Increasing their gain further to try to achieve better performance will result in a reduction in stability margins, a more oscillatory closed-loop responses, and ultimately worse performance.

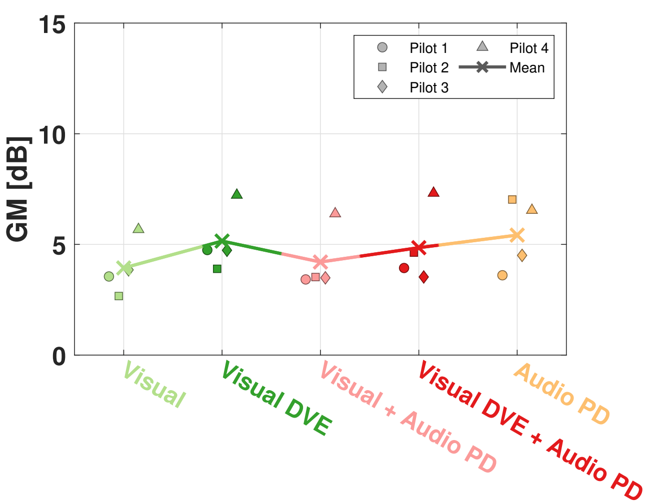

Fig. 20: Identified open-loop PVS gain margin

Test Pilot Qualitative Feedback

This section reports the feedback from the test subject who is a test pilot. The same test pilot provided comments on the use of full-body haptic feedback in Ref. 5). The test pilot added the below comments about the use of 3-D audio cueing:

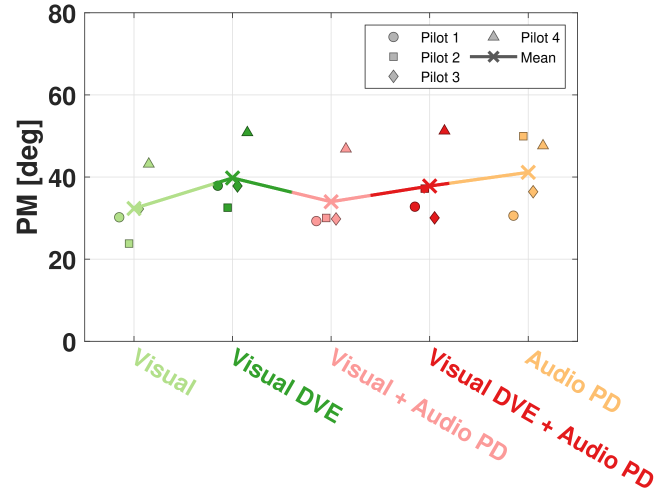

Fig. 21: Identified open-loop PVS phase margin.

1. The sounds were slightly confusing at the beginning but after a while it became understandable.
2. The frequency levels were distinguishable against the attitude error and error rate. Also, the decreasing in the inter-pulse interval was noticeable as the error increase rapidly. The high pitch was very helpful when exceeding the adequate error tolerance as an alert after a warning.
3. The 3-D audio were very helpful in degraded vision with foggles to know the initial direction of the error and its rate. With spatial audio one can immediately move the stick based on what direction and frequency are heard when the visuals are not clear enough to trust.
4. Sometimes the direction switched very quickly between left and right and accompanied with high frequency giving the impression of doing bad tracking but in fact that is not necessarily correct. That is because the rate feedback can change very fast according to the sum of sines signal.
5. The sound occurs at zero or low errors (when the indicator is at or close to the reference) is slowly changing and the bass (low frequency) is not motivating enough to move the stick and the pilot may wait and put the focus on larger error signals. This harms the desired success rate. However, if the sound was quicker and higher, the pilot may overshoot than the needed stick action.

CONCLUSIONS

Spatial audio cueing algorithms were developed, implemented, and tested for augmented pilot perception. These audio cueing algorithms are based on 3-D audio obtained via a commercial, off-the-shelf closed-ear headset. Cueing algorithms were developed for roll-axis compensatory tracking tasks where the pilot acts on the displayed error between a desired input and the comparable vehicle output motion to produce a control action. The tracking error was displayed to the pilot using three different cueing modalities: visual, audio, and combined visual and audio. For the visual and combined visual and audio modalities, visual cues were also considered in degraded visual environments (DVE). Experiments that involved four test subjects, one of which was a test pilot, were conducted to gather quantitative data and qualitative feedback for analyzing the performance of the audio cueing algorithms. Time- and frequency-domain analyses on the test data were performed.

Based on this work, spatial audio cueing algorithms that are based on a proportional-derivative (PD) compensation strategy on the tracking error were found to provide satisfactory PVS performance for the task in consideration when using audio feedback only (no visual cues) and to improve PVS performance, especially in degraded visual environment (DVE) when using combined visual and audio feedback. These results indicate that the use of secondary sensory cues such as 3-D sounds to augment the vehicle perception can lead to improved/partially-restored PVS performance when primary sensory cues like vision are impaired or denied. These results are largely in agreement with previous studies involving full-body haptic cueing (Ref. 5).

Future work will focus on extending the haptic and audio cueing algorithms to aggressive and non-aggressive tasks with the varying dynamic characteristics of the aircraft (*e.g.*, response representative of Level 2 and Level 3 handling qualities), to other axes singularly (*e.g.*, pitch), and to multiple axes tracking tasks (*e.g.*, roll and pitch) with and without cross-coupling between the axes. Additionally, stabilization tasks for the roll axis only, pitch axis only, and combined roll and pitch axes will also be considered. Visual, full-body haptic, and spatial audio cueing will be combined to assess the interactional dynamics of these three sensory paths. The pilot workload will be estimated for each cueing modality using the approach in Ref. 10. All of these measures will be compared to address potential differences in pilot equalization and workload as a function of cueing strategy.

ACKNOWLEDGMENTS

This research was partially funded by the U.S. Government under agreements no. N000142312067. The views and conclusions contained in this document are those of the authors and should not be interpreted as representing the official policies, either expressed or implied, of the U.S. Combat Capabilities Development Command Aviation & Missile Center or the U.S. Government.

REFERENCES

[1]McGrath, B. J., "Tactile Instrument for Aviation," Technical report, NAMRL Monograph 49, Naval Aerospace Medical Research Laboratory, Pensacola, FL, 2000.

[2]McGrath, B. J., Estrada, A., Braithwaite, M. G., Raj, A. K., and Rupert, A. H., "Tactile Situation Awareness System Flight Demonstration," Technical report, Army Aeromedical Research Laboratory, Fort Rucker, AL, 2004.

[3]Wolf, F. and Kuber, R., "Developing a head-mounted tactile prototype to support situational awareness," *International Journal of Human-Computer Studies*, Vol. 109, 2018, pp. 54–67.
doi: 10.1016/j.ijhcs.2017.08.002

[4]Jennings, S., Cheung, B., Rupert, A., Schultz, K., and Craig, G., "Flight-Test of a Tactile Situational Awareness System in a Land-based Deck Landing Task," Proceedings of the Human Factors and Ergonomics Society 48th Annual Meeting, September 20-24, 2004.
doi: 10.1177/154193120404800131

[5]Morcos, M. T., Fishman, S. M., Cocco, A., Saetti, U., Berger, T., Godfroy-Cooper, M., and Bachelder, E. N., "Full-Body Haptic Cueing Algorithms for Augmented Pilot Perception in Degraded/Denied Visual Environments," Proceedings of the 79th Annual Forum of the Vertical Flight Society, West Palm Beach, May 15-18, 2023.
doi: 10.4050/F-0079-2023-18072

[6]McRuer, D. T., Clement, W. F., Thompson, P. M., and Magdaleno, R. E., "Minimum Flying Qualities. Volume 2: Pilot Modeling for Flying Qualities Applications," Technical report, Systems Technology, Inc Hawthorne, CA, 1990.

[7]Klyde, D. H., Ruckel, P., Pitoniak, S. P., Schulze, P. C., Rigsby, J., Xin, H., Brewer, R., Horn, J., Fegely, C. E., Conway, F., Ott, C. R., Fell, W. C., Mulato, R., and Blanken, C. L., "Piloted Simulation Evaluation of Tracking MTEs for the Assessment of High-Speed Handling Qualities," Proceedings of the 74th Annual Forum of the American Helicopter Society, May 14-17, 2018.

[8]Hess, R. A., "Simplified approach for modelling pilot pursuit control behaviour in multi-loop flight control tasks," *Proceedings of the Institution of Mechanical Engineers, Part G: Journal of Aerospace Engineering.*, Vol. 220, (2), 2006, pp. 85–102.
doi: 10.1243/09544100JAERO33

[9]McRuer, D. T. and Jex, H. R., "A Review of Quasi-Linear Pilot Models," *IEEE Transations on Human Factors in Electronics*, Vol. 8, (3), 1967, pp. 231–249.
doi: 10.1109/THFE.1967.234304

[10]Bachelder, E. N. and Godfroy-Cooper, M., "Pilot Workload Estimation: Synthesis of Spectral Requirements Analysis and Weber's Law," AIAA 2014-1467, AIAA SciTech Forum, January 7-11, 2019.
doi: 10.2514/6.2019-1228

[11]Godfroy-Cooper, M., Miller, J. D., Bachelder, E. N., and Wenzel, E. M., "Isomorphic Spatial Visual-Auditory Displays for Operations in DVE for Obstacle Avoidance," Proceedings of the 44th Annual Forum of the European Rotorcraft Forum, Delft, Netherlands, September 19-20, 2018.
doi: 10.4050/F-0075-2019-14563

[12]Tischler, M. B. and Rample, R. K., *Aircraft and Rotorcraft System Identification: Engineering Methods and Flight Test Exemples, Second Edition*, Princeton University Press, Princeton, NJ, 1972.

[13]McRuer, D., Graham, D., and Reisener, W., "Human Pilot Dynamics in Compensatory Systems," Technical report, AFFDL-TR-65-15, Air Force Flight Dynamics Laboratory, Air Force Systems Command, Wright-Patterson Air Force Base, OH, Redstone Arsenal, AL, 1965.

[14]Anon, "Aeronautical design standard performance specification handling qualities requirements for military rotorcraft," Technical report, U.S. Army Aviation and Missile Command Aviation Engineering Directorate, Redstone Arsenal, AL, 2000.